ISSN: 2278-5213

RESEARCH ARTICLE

Unsteady Convective Boundary Layer Flow of a Nano Fluid over a Stretching Surface in the Presence of a Magnetic Field, Dissipation and Non-uniform Heat sources

Y. Madhusudhana Reddy
Department of Mathematics, Sri Venkateswara Institute of Technology, Anantapuramu, A.P., India
ymsmadhu@gmail.com

Abstract

The unsteady convective flow of a nanofluid over a stretching surface with variable transport properties and radiation effect in the presence of heat source has been analyzed. The Oberbeck-Boussinesq approximation is used in the flow equations. The governing non-linear coupled partial differential equations have been solved by using Runge-Kutta fourth order method with shooting technique. The effects of several governing parameters on flow variables viz. velocity, temperature, nanofluid volume fraction have been discussed. It is observed that the thickness of the momentum and thermal boundary layers decrease with an increase in the unsteady parameter. Velocity and temperature enhance with radiation, Brownian motion, thermophoresis parameters and reduce with Prandtl number. Concentration decreases with Lewis number.

Keywords: Stretching surface, magnetic field, dissipation, nanofluid volume fraction, Prandtl number.

Introduction

The fluid flow due to a stretching surface has importance applications such as extrusion, melt-spinning, fiber coating, manufacture of plastic and rubber sheets, design of heat exchangers and equipment for chemical processing. The study of boundary layer flow of an electrically conducting fluid finds its applications in cooling of electronic devices, fans, nuclear reactors during emergency shutdown, textile and paper industries, glass-fiber production, the utilization of geothermal energy, the thermal boundary layer control in the field of aerodynamics, plasma studies, food processing, etc. Sakiadis (1961) is the pioneer to study boundary layer flow of a Newtonian fluid owing to the stretching of an elastic flat sheet that moves in its own plane with velocity varying linearly with distance from a fixed point due to the applied stress. Following this study several researchers (Gupta and Gupta, 1977; Grubkha and Bobba, 1985; Vajravelu, 1994) attempted to analyze the heat and mass transfer aspects in Newtonian/non-Newtonian fluids considering different physical conditions. In the recent years the study of heat transfer in nanofluids attracted the attention of researchers due to the fact that conventional heat transfer fluids such as water, oil, ethylene glycol mixture are poor heat transfer liquids. Hence, several methods have been developed to enhance the thermal conductivity of these liquids and the enhancement is achieved by the suspension of nano particles of materials in liquids (Kakac and pramuanjaroenkij, 2006). The word “nanofluid” was coined by Choi (1996). Nanofluids are fluids that contain small volumetric quantities of nanometer-sized particles, called nanoparticles. These particles are usually made from metals such as aluminum, copper, gold, iron and titanium or their oxides. The base fluids used are water, oil, ethylene glycol, toluene etc.

Khan and Pop (2010) made a numerical study of the boundary layer flow of a nanofluid past a stretching sheet and they analyzed the effects of Brownian motion and thermophoresis. Kuznestov and Nield (2009) investigated the influence of nanoparticles on natural convection boundary layer flow past a vertical plate. Bachok *et al*. (2010) analyzed the steady boundary layer flow of a nanofluid past a moving semi-infinite flat plate in a uniform free stream. Hamad and Pop (2011) discussed the boundary layer flow near the stagnation–point on a permeable stretching sheet in a porous medium saturated with a nanofluid. The flow and heat transfer problems in reality have unsteady nature owing to the sudden stretching of the sheet owing to the impulsively stretching of the surfaces with certain velocity the in viscid flow is developed instantaneously but the flow in the viscous layer in the vicinity of the sheet is developed slowly and it becomes a fully developed flow after a certain instant of time. Several authors (Vajravelu 1994; Hayat *et al.,* 2008; Jafar *et al.,* 2011;, Chamkha *et al.,* 2011; Mukhopadhyay, 2011; Bhattacharyya *et al.,* 2011) analyzed the problem of unsteady stretching surface under different physical situations by introducing similarity variables to transform the governing time dependent boundary layer equations into the ordinary differential equations. Elbashbeshy and Bazid (2003) studied the unsteady flow over a stretching sheet by obtaining the similarity solutions for the boundary layer equations. This study was extended by Abd El-Azi (2009) for some realistic phenomena. Mukhopadhyay (2011) analyzed the combined effects of slip and suction/blowing on unsteady mixed convection flow past a stretching sheet. In a subsequent study they obtained a similarity solution for the unsteady two-dimensional fluid in the presence of first order chemical reaction.

©Youth Education and Research Trust (YERT)

The study of magnetic field in nanofluids has several applications which are concerned with cooling of nuclear reactors by liquid sodium and induction flow meter which depends on the potential difference in the fluid in the direction perpendicular to the motion and to the magnetic field (Ganesan and palani, 2004). It is reported that during the process of chemotherapy, failure to provide localized drug targeting resulted in the increase of toxic effects on neighboring organs and tissues, while the process of localized drug therapy is achieved by magnetic drug targeting. This technology is based on binding established anticancer using magnetic nanoparticles which concentrate the drug in the vicinity of the tumor through magnetic fields. The application of MHD in the polymer industry and metallurgy has attracted the attention of many researchers (Ishak, 2010; Ali *et al.,* 2011; Makinde, 2012). In many fluid particle flows, the fluid heat generation or absorption and the thermal radiation effects may play an important role in altering the heat transfer characteristics. There has been a renewed interest in studying MHD flow and heat transfer in porous and non-porous media due to the effect of magnetic fields on the boundary layer flow control and on the performance of many systems using electrically conducting fluids. This effect is known as the Hall Effect. The study of MHD heat transfer with Hall currents has several engineering applications for example power generators, transmission lines, refrigeration coils, MHD accelerators, electric transformers etc. When a strong magnetic field is applied to an ionized gas with low density, the conductivity normal to the magnetic field is reduced owing to the free spiralling of electrons and ions around the magnetic lines of force and the current is induced in the normal direction to the electric and magnetic fields. The effect of Hall current on MHD free convection flow past a semi-infinite vertical plate with mass transfer and a nano-Newtonian power law fluid over a stretching surface by several researchers (Abo-Eldahab and Abd El-Aziz, 2000; Abo-Eldahab and Elbarbary, 2001; Abo-Eldahab and Salem, 2004; Abd El-Aziz, 2010; Ali et al., 2011). In this paper, the unsteady convective flow of a nanofluid over a stretching surface with variable transport properties and radiation effect in the presence of heat source has been analyzed. The Oberbeck-Boussinesq approximation is used in the flow equations. The governing non-linear coupled partial differential equations have been solved by using Runge-Kutta fourth order method with shooting technique. The effects of several governing parameters on flow variables viz. velocity, temperature, nanofluid volume fraction have been discussed. It is observed that the thickness of the momentum and thermal boundary layers decrease with an increase in the unsteady parameter. Velocity and temperature enhance with radiation, Brownian motion, thermophoresis parameters and reduce with Prandtl number. Concentration decreases with Lewis number. The skin friction, Nusselt number and Sherwood number on the stretching sheet have been calculated and discussed.

Formulation of the Problem

Consider the unsteady two-dimensional boundary layer flow of a nanofluid past a stretching sheet coinciding with the plane y = 0. We choose the Cartesian co-ordinate system with its origin located at the leading edge of the sheet with the positive x-axis extending along the sheet in the upward direction and the y-axis is taken normal to the surface of the sheet and is positive in the direction from the sheet to the fluid (Fig. 1).

Fig. 1. Physical Model and coordinate system.

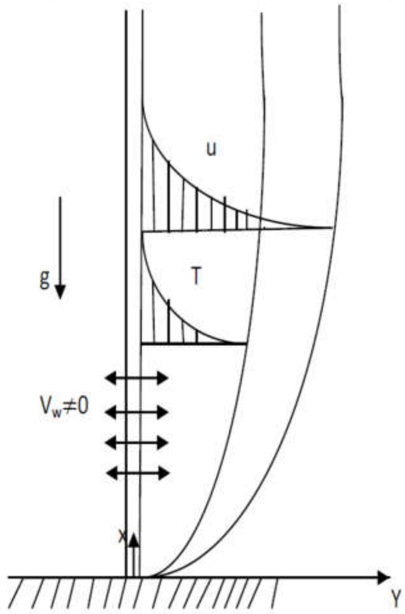

We consider that an external constant magnetic field B0 is applied in the positive y–direction. The temperature and the nanoparticle fraction are maintained at prescribed constant values Tw and Cw on the sheet while the ambient fluid has a uniform temperature T∞ and concentration C∞. Taking Hall effects into account and assuming that the electronic pressure is neglected and no electric field is imposed on the flow field, the generalized Ohm's law that includes Hall current can be written as

$$\bar{J} = \sigma(\bar{E} + \bar{V}x\bar{B} - \frac{1}{en_e})x\bar{B} + \frac{1}{en_e}\nabla p_e$$

Where $\bar{J} = (J_x J_y, J_z)$ is the current density vector, E is the intensity vector of the electric field, V is the velocity vector, $\bar{B} = (0, B_0, 0)$ the magnetic induction vector, $\sigma(= e^2 n_e t_e / m_e)$ is the electrical conductivity,τe is the electron collision time is the charge of electronic is the number of density of electrons, me is mass of the electrons and Pe the electron pressure .The equation of conservation of electron charge $\nabla.\bar{J} = 0$ results $j_y = cons\tan t$,this indicates that $j_y = 0$ everywhere in the flow .

Hence above equation reduces to

$$j_x = \frac{\sigma B_0}{1+m^2}(mu - w)$$

$$j_z = \frac{\sigma B_0}{1+m^2}(u + mw) \qquad (1)$$

Here u,v and w are the components of the velocity vector V,m=(=$\omega_e \tau_e$) is the Hall parameter,ω e is the electron frequency.

We assume that the nanofluid is isotropic and homogeneous and has the constant viscosity and electric conductivity. Under these assumptions, the boundary layer equations governing this MHD flow, heat and mass transfer of nanofluids with Hall Effect using Boussinesq approximation are

$$\frac{\partial u}{\partial t} + u\frac{\partial u}{\partial x} + v\frac{\partial u}{\partial z} = \nu\frac{\partial^2 u}{\partial y^2} + \beta g(T - T_\infty) + \beta^* g(C - C_\infty) - (\frac{\mu}{k})u - \\ -\frac{\sigma B_0^2}{\rho(1+m^2)}(u + mw) \qquad (2)$$

$$\frac{\partial w}{\partial t} + u\frac{\partial w}{\partial x} + v\frac{\partial w}{\partial y} = \nu\frac{\partial^2 w}{\partial y^2} + \frac{1}{\rho_e}[(1 - C_\infty)\rho_{f_\infty}\beta g(T - T_\infty)] - \frac{(\rho_p - \rho_{f_\infty})g(C - C_\infty)}{\rho_f} - \\ -(\frac{\mu}{k})w - \frac{\sigma B_o^2}{1+m^2}(mu - w) \qquad (3)$$

The energy equation is

$$\rho C_p(\frac{\partial T}{\partial t} + u\frac{\partial T}{\partial x} + v\frac{\partial T}{\partial y}) = k_f(\frac{\partial^2 T}{\partial y^2}) + q''' + \mu[(\frac{\partial u}{\partial y})^2 + (\frac{\partial w}{\partial y})^2] + \\ +2\mu((\frac{\partial u}{\partial y})^2 + (\frac{\partial w}{\partial y})^2) + \sigma B_o^2(u^2 + w^2) + Q_1^{'}(C - C_\infty) - (\frac{\partial q_R}{\partial y}) \qquad (4)$$

The diffusion equation is

$$(\frac{\partial C}{\partial t} + u\frac{\partial C}{\partial x} + v\frac{\partial C}{\partial y}) = D_B(\frac{\partial^2 C}{\partial y^2}) - k_c(C - C_\infty) + \frac{D_m K_T}{T_m}(\frac{\partial^2 t}{\partial y^2}) \qquad (5)$$

The coefficient q''' is the rate of internal heat generation (>0) or absorption(<0). The internal heat generation /absorption q''' is model as

$$q''' = \left(\frac{ku_s}{x\nu}\right)\left[A1\left(T_w - T\infty\right)f'(\eta) + B1\left(T - T\infty\right)\right] \qquad (6)$$

Where A1 and B1 are coefficients of space dependent and temperature dependent internal heat generation or absorption respectively. It is noted that the case A1>0 and B1>0, corresponds to internal heat generation and that A1<0 and B1<0, the case corresponds to internal heat absorption case.

The radiation heat term by using the Rosseland approximation is given by

$$q_r = -\frac{4\sigma^\bullet}{3\beta_R}\frac{\partial T'^4}{\partial y}, \quad T'^4 \cong 4TT_\infty^3 - 3T_0^4, \quad \frac{\partial q_R}{\partial z} = -\frac{16\sigma^\bullet T_0^3}{3\beta_R}\frac{\partial^2 T}{\partial y^2} \qquad (7)$$

Where $\sigma^\bullet$ is the Stefan-Boltzman constant ands β_R mean absorption coefficient.

Using (7) equation (4) reduces to

$$\rho C_p(\frac{\partial T}{\partial t} + u\frac{\partial T}{\partial x} + v\frac{\partial T}{\partial y}) = k_f(\frac{\partial^2 T}{\partial y^2}) + [A1(T_w - T_\infty) + B1(T - T_\infty] + \\ +2\mu[(\frac{\partial u}{\partial y})^2 + (\frac{\partial w}{\partial y})^2] + \sigma B_o^2(u^2 + w^2) + Q_1^{'}(C - C_\infty) + \frac{16\sigma^\bullet T_\infty^3}{3\beta_R}(\frac{\partial^2 T}{\partial y^2}) \qquad (8)$$

where T is the temperature and C is the concentration in the fluid. k_f is the thermal conductivity, Cp is the specific heat at constant pressure, β is the coefficient of thermal expansion, $\beta^\bullet$ is the volumetric expansion with concentration, Q_1^1 is the radiation absorption coefficient, q_r is the radiative heat flux, kc is the chemical reaction coefficient, D_B is the molecular viscosity, D_m is the mass diffusivity coefficient, K_T is the thermal temperature ratio, T_m mean temperature of the fluid, k is the porous permeability parameter.

The boundary conditions for this problem can be written as

$$u = U(x,t) + L\frac{\partial u}{\partial y}, v = V_w(x,t), w = 0, T = T_w, C = C_w \quad at \quad y = 0 \tag{9}$$

$$u = w = 0, T = T_\infty, C = C_\infty \qquad as \quad y \to \infty$$

Where u and v are the fluid velocity components along x and y-axis respectively and t is the time. $v_w(x,t) = -(\frac{\nu U w}{x})^{1/2} f(0)$ represents the mass transfer at the surface with Vw>0 for injection and Vw>0 for suction .The flow is caused by the stretching of the sheet which moves in its own plane with the surface velocity $U_w(x,t) = \frac{ax}{(1-ct)}$, where a (stretching rate) and c are the positive constants having dimension time^{-1} (with t<1,c≥0).It is noted that the stretching rate $\frac{a}{(1-ct)}$ increases with time ,since a>0.The surface temperature and concentration of the sheet varies with the distance x from the slot and time t in the form so that surface temperature $T_w(x,t) = T_\infty + \frac{ax^2}{2\nu(1-ct)^{3/2}}$ and surface concentration $C_w(x,t) = C_\infty + \frac{ax^2}{2\nu(1-ct)^{3/2}}$ where a≥0 .q_w and m are the heat and mass flux.

The particular form of $U_w(x,t), T_w(x,t)\, and\, C_w(x,t)$ has been chosen in order to derive a similarity transformation which transforms the governing partial differential equations (2)-(5) into a set of highly nonlinear ordinary differential equations.

The stream function ψ(x,t) is defined as:

$$u = \frac{\partial\psi}{\partial y} = \frac{ax}{(1-ct)} f'(\eta), v = -\frac{\partial\psi}{\partial x} = \frac{a\nu}{\sqrt{(1-ct)}} f(\eta) \tag{10}$$

On introducing the similarity variables

$$\eta = \sqrt{\frac{a}{(1-ct)}}\, y \tag{11}$$

$$\psi(x,y,t) = (\frac{\nu a}{1-ct})^{1/2} x f(\eta), w = (\frac{ax}{1-ct}) g(\eta) \tag{12}$$

$$T(x,y,t) = T_\infty + \frac{ax^2}{2\nu(1-ct)^{3/2}}\theta(\eta), \theta(\eta) = \frac{T-T_\infty}{T_w - T_\infty} \tag{13}$$

$$C(x,y,t) = C_\infty + \frac{ax^2}{2\nu(1-ct)^{3/2}}\phi(\eta), \phi(\eta) = \frac{T-T_\infty}{T_w - T_\infty} \tag{14}$$

$$B^2 = B_o^2(1-ct)^{-1} \tag{15}$$

Using equations (11)- (15) into equations(2),(3.),(5)and (8) we get

$$\begin{aligned} f''' + f f'' - f'^2 - S(f' + 1.5 f'') + G(\theta + N\varphi) - D^{-1} f' - \\ - \frac{M^2}{1+m^2}(f' + mg) = 0 \end{aligned} \tag{16}$$

$$\begin{aligned} g'' + fg' - f'g - S(g' + 1.5g'') - D^{-1} g + \\ + \frac{M^2}{1+m^2}(mf' - g) = 0 \end{aligned} \tag{17}$$

$$(1+\frac{4Nr}{3})\theta''+\Pr(f\,\theta'-2f'\theta-0.5S(3\theta+\eta\,\theta')+\Pr(A1f'+B1\theta)+$$
$$+\Pr Nb\theta'\phi'+\Pr Nt(\theta')^2+Ec((f'')^2+(g')^2)+\frac{M^2}{1+m^2}(f'^2+g^2)+Q1\phi \quad (18)$$

$$\phi''+Le(f\phi'-2f'\phi-0.5S(3\phi+\eta\phi')-Le\gamma\phi+Le(\frac{Nt}{Nb})\theta''=0 \quad (19)$$

where S=c/a is the unsteadiness parameter.

$M=\frac{\sigma B_0^2}{\rho a}$ is the magnetic parameter, $G=\frac{\beta g(T_w-T_\infty)}{U_w v_w^2}$ is the thermal buoyancy parameter, $N=\frac{\beta^*(C_w-C_\infty)}{\beta(T_w-T_\infty)}$ is the buoyancy ratio, $\Pr=\frac{\mu C_p}{k_f}$ is the Prandtl number, $Ec=\frac{U_w^2}{C_P(T_w-T_\infty)}$ is the Eckert number, $Q_1=\frac{\nu Q_1'}{v_w^2}$ is the Radiation absorption parameter, $Sc=\frac{\nu}{D_B}$ is the Schmidt number, $Nr=\frac{4\sigma^\bullet T_\infty^3}{\beta_R k_f}$ is the Radiation parameter

$m=\omega_e\tau_e$ is the Hall parameter, $\gamma=\frac{k_o\nu}{v_w^2}$ is the chemical reaction parameter

$Nb=\frac{(\rho C)_p D_B(C_w-C_\infty)}{\nu(\rho C)_f}$, (Brownian motion parameter)

$Nt=\frac{(\rho C)_p D_T(T_w-T_\infty)}{\nu(\rho C)_f T_\infty}$, (Thermophoresis motion parameter)

$Le=\frac{\nu}{D_B}$, (Lewis number), $A=L(\frac{ax}{1-ct})'^{1/2}$ (Slip parameter)

$N_2=\frac{3}{3+4Nr}, P_1=\Pr N_2$

It is pertinent to mention that γ>0 corresponds to a degenerating chemical reaction while γ<0 indicates a generation chemical reaction.

The transformed boundary conditions (6.2.9) reduce to

$$f'(0)=1+Af''(0), f(0)=f_w, \theta=1, \phi=1 \; at \; \eta=0 \quad (20)$$
$$f'(\infty)\to 0, g(\infty)\to 0, \theta(\infty)\to 0, \phi(0)\to 0 \quad (21)$$

Where $fw=\frac{v_w}{\sqrt{a\nu}}$ is the mass transfer coefficient such that fw>0 represents suction and fw<0 represents injection at the surface.

Skin friction, Nusselt number and Sherwood number

The physical quantities of engineering interest in this problem are the skin friction coefficient Cf, the Local Nusselt number Nux , the Local Sherwood number Shx which are expressed as

$$\frac{1}{2}C_f\big)R_{ex}=f''(0),\ \frac{1}{2}C_{fz}\big)R_{ez}=g'(0),$$
$$Nux/\big)R_{ex}=1/\theta(0)\ ,\ Shx/\big)R_{ex}=1/\phi(0)$$

Where μ is the dynamic viscosity of the fluid and Rex is the Reynolds number.

For the computational purpose and without loss of generality ∞ has been fixed as 8. The whole domain is divided into 11 line elements of equal width, each element being three nodded.

Results and discussion

The non-linear ordinary differential equations (16)–(19) subject to the boundary conditions (20) & (21) are solved numerically using the shooting technique. In order to verify the validity and accuracy of the numerical scheme applied in the present analysis, results for the heat transfer rate $-\theta'$ 0 for different values of Prandtl number have been compared with the published results of Grubka and Bobba (1985) and Ali (1994) for regular viscous fluid over a linearly stretching sheet in the absence of magnetic field (M=0), Hall current (m=0). The results are found to be in good agreement as presented in Table (1). The results for different governing parameters, viz. unsteady parameter S, free convection parameter G , buoyancy ratio N, radiation parameter Nr, Prandtl number Pr, Brownian motion parameter Nb, thermophoresis parameter Nt, heat source parameters A1,B1, radiation absorption parameter Q1 , Lewis number Le on the flow variables are discussed. To judge the accuracy of the computed numerical results, results of the present analysis are compared with the already published results for the steady case (S = 0) and Newtonian fluid case. In particular the numerical values of Nusselt number on wall are presented in Table 1 and are found to be in good agreement.

Table 1. Comparison.

S	G	Pr	Grubka and Bobba (1985)	Ali (1994)	Ishak (2010)	Present Results
		0.01	0.0197	-	0.0197	0.019745
		0.72	0.8086	0.8058	0.8086	0.808676
		1.0 0	1.0000	0.9961	1.0000	1.000473
0.0	0.0	3.00	1.9237	1.9144	1.9237	1.923425
		10.0	3.7207	3.7006	3.7207	3.720554
		100.0	12.2940	-	12.2941	12.293801
1.0	0.0	1.0	-	-	1.6820	1.681997
	1.0		-	-	1.7039	1.703922
	1.0		-	-	1.0873	1.087063
0.0	2.0	1.0	-	-	1.1423	1.142197
	3.0		-	-	1.1853	1.185212

The effect of free convection parameter G on the velocity is depicted in Fig. 2a and b when N = 0.1, Pr = 1, Nb = 0.5, Nt = 0.5, Nr = 0.1, Le = 1, A1 = 0.1, B1=0.1,Q1=0.5,M = 0.5. From this figure it is observed that the velocities increase monotonically to zero as the distance η increases from the boundary. In the steady state case the velocity enhances from its peak value in the boundary layer and then reduces to zero in all the three cases. Physically the free convection parameter G>0 corresponds to the heating of the fluid (assisting flow), G<0 corresponds to cooling of the fluid (opposing flow) and G = 0 means the absence of free convection currents. An increase in G results in the enhancement of velocities due to the enhancement of convection currents and thus thickness of the boundary layer increases. It is also observed that when the surface is impermeable the velocity in the steady flow case reduces to zero faster. An increase in the value of G amounts to an increase in the temperature difference which leads to the enhancement of convection currents and thus facilitates to increase the velocities, consequently the thickness of the boundary layer increases. Fig. 3 illustrates the influence of magnetic field. It is observed that the presence of magnetic field reduces the primary velocity and enhances the secondary velocity throughout the boundary layer which is in the conformity with the fact that the Lorentz force or magnetic force acts as a retarding force. Higher the Lorentz force lesser is the velocity. This is true for steady and unsteady cases. An increase in Hall parameter (m) leads to an enhancement in the primary and secondary velocities (Fig. 4). The primary velocity (f') decreases, secondary velocity(g) increases for increasing values of buoyancy ratio (Fig. 5a and b) and hence a reduction in the thickness of the boundary layer is noticed. The velocities grow in the degenerating chemical reaction case (Fig.7). From Fig. 8, it is observed that for increasing values of suction parameter fw, the velocity (f') is decreasing while the secondary velocity(g) depreciates with fw>0 and enhances with fw<0 in the entire flow region. The velocities decrease for increasing values of space dependent heat source/sink parameter (A1) which is presented in Fig. 9. An increase in the heat generating/absorbing source (B1) depreciates both the velocities (Fig.10). It is observed that the unsteady parameter S results in the enhancement in the primary velocity in the flow region (0, 2), reduces it in the remaining region. These observations are consistently noticed or reflected in the values of shear stress. The secondary velocity (g) upsurges in the entire flow region with increase in S (Fig. 17a and b). From Fig.11a and b, we find that both the velocities depreciate with higher values of slip parameter (A).

From Fig.12a and b it is observed that the influence of Nt is to increase the velocities. The effect of Brownian motion parameter (Nb) on velocity is depicted in Fig. 13a and b. Increase in Nb enhances the velocities and hence the thickness of the hydrodynamic boundary layer decays. In the unsteady case the velocities decrease steadily. From Fig. 14a and b it is observed that the presence of radiation decreases the velocities. Further increase in the radiation parameter facilitates the depreciation of the velocities and thus decays the thickness of the boundary layer. The effect of Lewis number on velocities is depicted in Fig.15a and b. As Le increases from 1 to 2 there is an increase in the primary velocity and decreases the secondary velocity in unsteady flows. A similar behavior is noticed for steady and unsteady cases. With increase in the unsteady parameter (S) the velocities and the boundary layer thickness increase. The primary and secondary velocities experience enhancement with rising values of radiation absorption parameter (Q1). Fig.18a and b illustrates the effect of Prandtl number for a selected value of remaining parameters is to reduce the velocities leading to a reduction in the hydrodynamic boundary layer.

The variation of temperature (θ) and nanofluid volume fraction (ϕ) with Grashof number (G) shows that they depreciate with rising values of G in the flow region (2c and d). Higher the Lorentz force larger the temperature and reduces the nano-concentration in the flow region (3c and d).The temperature decreases and concentration enhances with higher values of Hall parameter(m) (Fig.4c and d). When the molecular buoyancy force dominates over the thermal buoyancy force the temperature depreciates while the nanofluid volume fraction increases when the buoyancy forces are in the same direction (Figs.5c and d). θ and ϕ experience an enhancement in both degenerating/generating chemical reaction cases (Fig.6c and d; 7c and d). It is observed that for increasing values of suction parameter (fw)the temperature increases while the nanofluid volume fraction enhances with suction(fw>0) and reduces with injection(fw<0)(Figs. 8c and d). An increase in space dependent heat source/sink(A1)/heat generating and absorbing source(B1) leads to an elevation in the temperature and nanofluid volume fraction in the entire flow region (Figs.9c and d; 10c and d). Higher the slip parameter (A) is larger the temperature and smaller the nanofluid volume fraction in the flow region (Figs.11c and d). Figure 14c and d presents the effect of radiation parameter on temperature and nanofluid volume fraction. Higher the radiative heat flux, larger the temperature and smaller the nanofluid volume fraction in the flow region. An increase in Lewis number (Le)/radiation absorption parameter (Q1) larger the temperature and nanofluid volume fraction. Thus, increase in Q1 leads to a growth in thermal and solutal boundary layer thickness. A rise in unsteady parameter (S)/ Prandtl number (Pr) reduces the temperature and enhances the nanofluid volume fraction in the flow region. Increasing values of Rd enhance the temperature leading to an increase in the thickness of the thermal boundary layer. In the unsteady case also the thermal boundary layer thickness is significantly increased with increasing values of Rd. The temperature steadily increases for an increase in Brownian motion parameter Nb in both steady and unsteady cases. From Fig. 13c and d it is observed that Nb increases the temperature and decreases the nano-concentration in the flow region. The effect of thermophoresis parameter Nt is depicted in Fig.12c and d. It is observed that the temperature increases and nano-concentration decreases for increasing values of Nt in the unsteady case.

The skin friction, Nusselt number and Sherwood number are tabulated in Table 2. From this table it is observed in the unsteady cases and increase in the free convection parameter (G) leads to an increase in both the skin friction components, Nusselt number and decreases the Sherwood number. The buoyancy ratio increases the values of skin friction (Cfx) ,Sherwood number, decreases the skin friction Cfz, Nusselt number on η=0. The effect of magnetic field is to enhance the skin friction components, Sherwood number, reduces the Nusselt number. A rise in Hall parameter (m) reduces Cfx, Nu Sh and enhances Cfz. The radiation parameter enhances the values of skin friction Cfx, Nu and reduces Cfz, Sh on the wall. The effect of Brownian motion parameter (Nb) on the skin friction Cfx, Nusselt number and Cfz is to decrease. This is due to the enhancement in velocity and temperature and reduction in the concentration. The thermophoresis parameter decreases the values of skin friction, Nusselt number and enhances Sherwood number. The effect of Prandtl number is to reduce the skin friction Cfz, Sherwood number and enhance the Nusselt number. Cfx, Nu enhances, Cfz, Sh reduces in both degenerating/generating chemical reaction cases. Cfx., Cfz,Nu grow, Sh decays with suction/injection parameter (fw) on the wall. Cfx, Cfz, Sh grow, Nu decays with unsteady parameter(S) on η=0.Lesser the thermal diffusivity larger Cfx, Nu, smaller Cfz, Sh on the wall. An increase in A1/B1, enhances Cfx, Nu and reduces Cfz, Sh on η=0.An increase in slip parameter (A) reduces the skin friction components, Nu and enhances Sh on the wall. Higher the value of radiation absorption parameter (Q1)/Lewis number (Le). Smaller Cfx, Nu and larger Cfz, Sh on the wall.

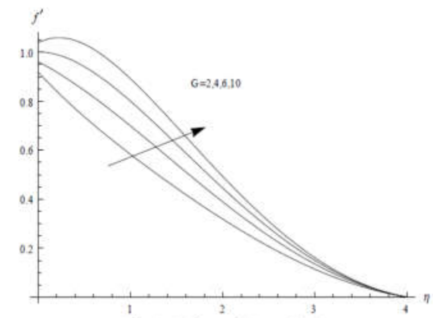

Fig.2a Effect of G on $f'(\eta)$
M=0.5,m=0.5,N=0.5,γ=0.5,Nr=0.5,Nt=0.5,Nb=0.5,Q1=0.5,
A1=0.1,B1=0.1,fw=0.2,A=0.2,Le=2,Pr=0.71

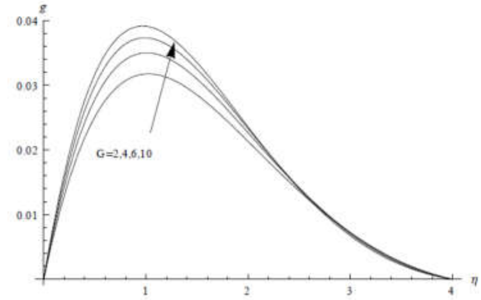

Fig.2b Effect of G on g(η)
M=0.5,m=0.5,N=0.5,γ=0.5,Nr=0.5,Nt=0.5,Nb=0.5,Q1=0.5,
A1=0.1,B1=0.1,fw=0.2s=0.1,A=0.2Le=2Pr=0.71

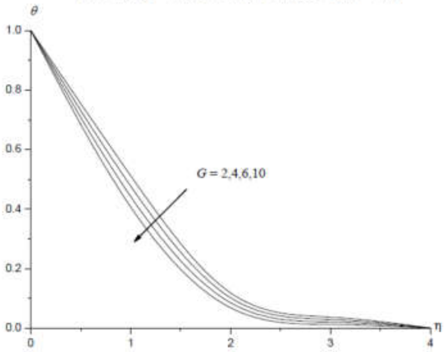

Fig.2c Effect of G on θ(η)
M=0.5,m=0.5,N=0.5,γ=0.5,Nr=0.5,Nt=0.5,Nb=0.5,Q1=0.5,
A1=0.1,B1=0.1,fw=0.2s=0.1,A=0.2Le=2Pr=0.71

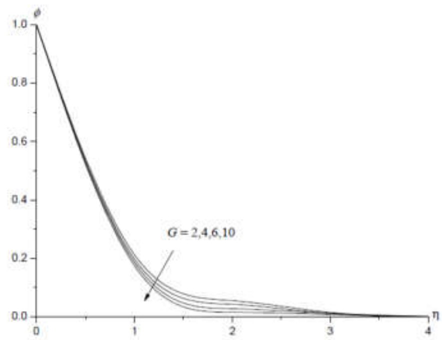

Fig.2d Effect of G on ϕ(η)
M=0.5,m=0.5,N=0.5,γ=0.5,Nr=0.5,Nt=0.5,Nb=0.5,Q1=0.5,
A1=0.1,B1=0.1,fw=0.2s=0.1,A=0.2Le=2Pr=0.71

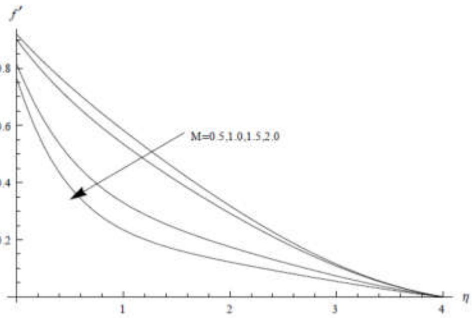

Fig.3a Effect of M on f' (η)
G=2,m=0.5,N=0.5,γ=0.5,Nr=0.5,Nt=0.5,Nb=0.5,Q1=0.5,
A1=0.1,B1=0.1,fw=0.2,s=0.1,A=0.2,Le=2,Pr=0.71

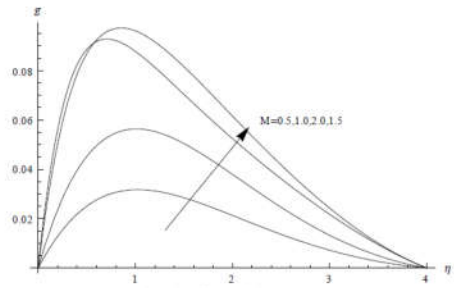

Fig.3b Effect of M on g(η)
G=2 m=0.5,N=0.5,γ=0.5,Nr=0.5,Nt=0.5,Nb=0.5,Q1=0.5,
A1=0.1,B1=0.1,fw=0.2s=0.1,A=0.2Le=2Pr=0.71

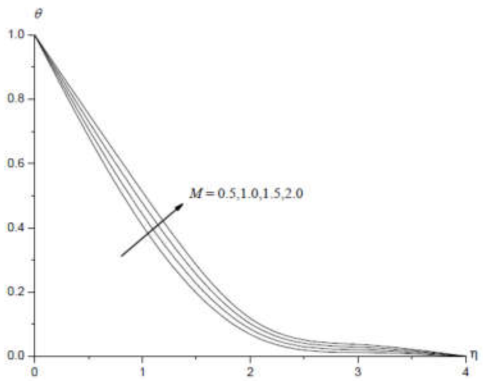

Fig.3c Effect of M on θ(η)
G=2 m=0.5,N=0.5,γ=0.5,Nr=0.5,Nt=0.5,Nb=0.5,Q1=0.5,
A1=0.1,B1=0.1,fw=0.2s=0.1,A=0.2Le=2Pr=0.71

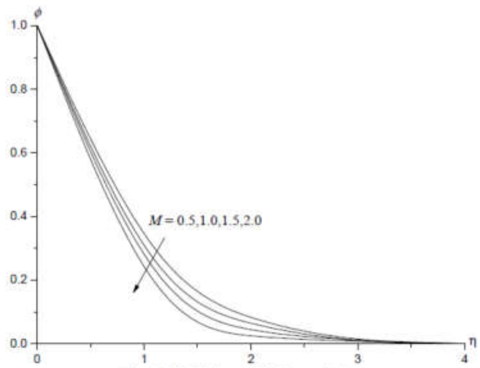

Fig.3d Effect of M on ϕ(η)
G=2 m=0.5,N=0.5,γ=0.5,Nr=0.5,Nt=0.5,Nb=0.5,Q1=0.5,
A1=0.1,B1=0.1,fw=0.2s=0.1,A=0.2Le=2Pr=0.71

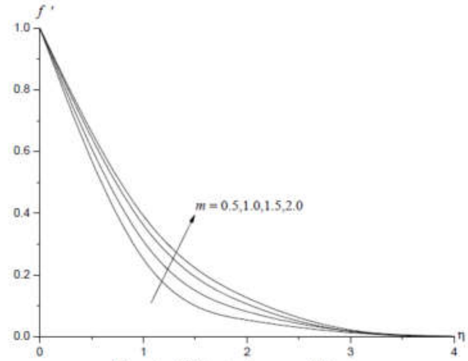

Fig.4a Effect of m on $f'(\eta)$
G=2,M=0.5, N=0.5,γ=0.5,Nr=0.5,Nt=0.5,Nb=0.5,Q1=0.5, A1=0.1,B1=0.1,fw=0.2,s=0.1,A=0.2,Le=,2Pr=0.71

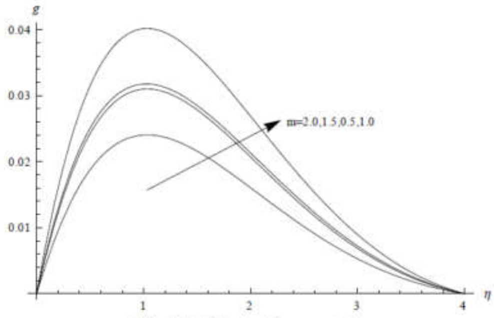

Fig.4b Effect of m on g(η)
G=2M=0.5, N=0.5,γ=0.5,Nr=0.5,Nt=0.5,Nb=0.5,Q1=0.5, A1=0.1,B1=0.1,fw=0.2s=0.1,A=0.2Le=2Pr=0.71

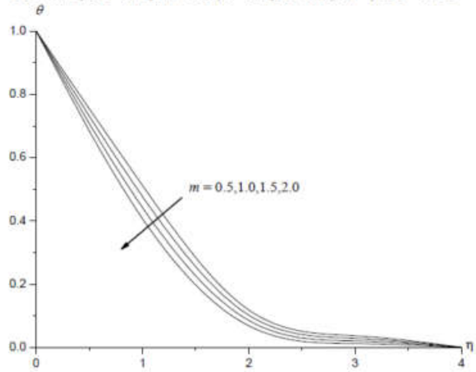

Fig.4c Effect of m on θ(η)
G=2M=0.5, N=0.5,γ=0.5,Nr=0.5,Nt=0.5,Nb=0.5,Q1=0.5, A1=0.1,B1=0.1,fw=0.2,s=0.1,A=0.2,Le=2,Pr=0.71

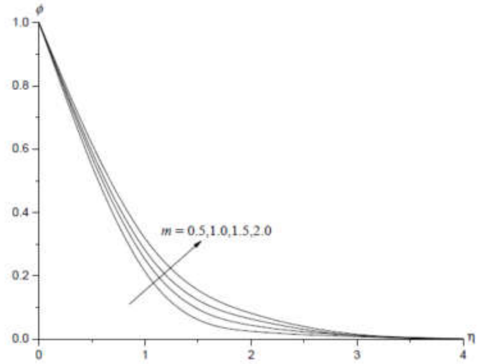

Fig.4d Effect of m on ϕ(η)
G=2M=0.5, N=0.5,γ=0.5,Nr=0.5,Nt=0.5,Nb=0.5,Q1=0.5, A1=0.1,B1=0.1,fw=0.2s=0.1,A=0.2Le=2Pr=0.71

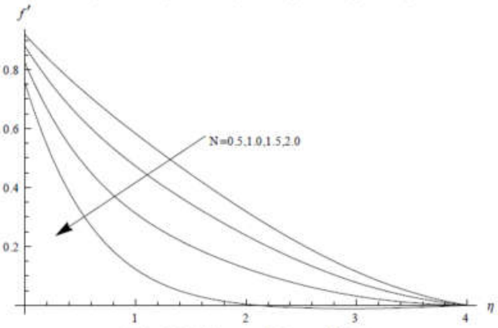

Fig.5a Effect of N on $f'(\eta)$
G=2,M=0.5,m=0.5,γ=0.5,Nr=0.5,Nt=0.5,Nb=0.5,Q1=0.5, A1=0.1,B1=0.1,fw=0.2,s=0.1,A=0.2,Le=2,Pr=0.71

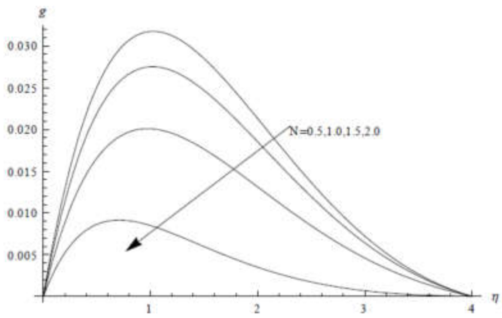

Fig.5b Effect of N on g(η)
G=2M=0.5,m=0.5, γ=0.5,Nr=0.5,Nt=0.5,Nb=0.5,Q1=0.5, A1=0.1,B1=0.1,fw=0.2s=0.1,A=0.2Le=2Pr=0.71

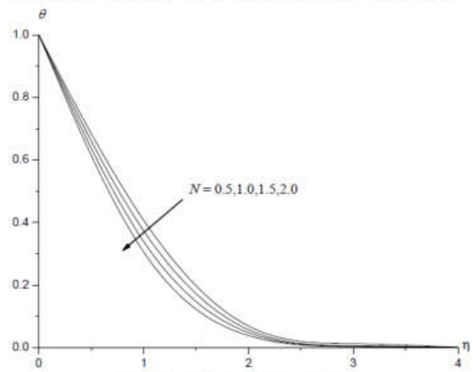

Fig.5c Effect of N on θ(η)
G=2M=0.5,m=0.5, γ=0.5,Nr=0.5,Nt=0.5,Nb=0.5,Q1=0.5, A1=0.1,B1=0.1,fw=0.2s=0.1,A=0.2Le=2Pr=0.71

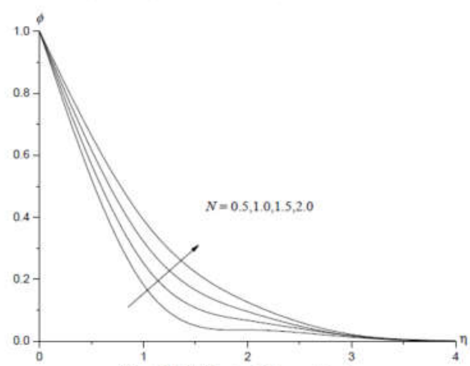

Fig.5d Effect of N on ϕ(η)
G=2M=0.5,m=0.5, γ=0.5,Nr=0.5,Nt=0.5,Nb=0.5,Q1=0.5, A1=0.1,B1=0.1,fw=0.2s=0.1,A=0.2Le=2Pr=0.71

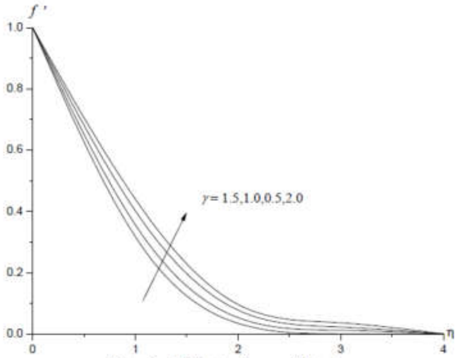

Fig.6a Effect of γ on $f'(\eta)$
G=2,M=0.5,m=0.5,N=0.5,Nr=0.5,Nt=0.5,Nb=0.5,Q1=0.5, A1=0.1,B1=0.1,fw=0.2,s=0.1,A=0.2,Le=2,Pr=0.71

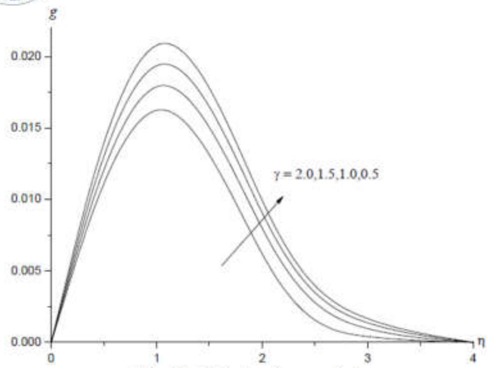

Fig.6b Effect of γ on g(η)
G=2M=0.5,m=0.5,N=0.5,Nr=0.5,Nt=0.5,Nb=0.5,Q1=0.5, A1=0.1,B1=0.1,fw=0.2s=0.1,A=0.2Le=2Pr=0.71

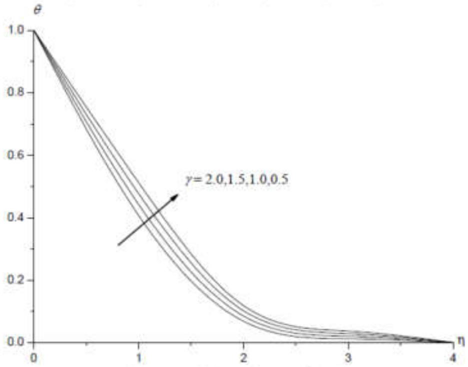

Fig.6c Effect of γ on θ(η)
G=2M=0.5,m=0.5,N=0.5,Nr=0.5,Nt=0.5,Nb=0.5,Q1=0.5, A1=0.1,B1=0.1,fw=0.2s=0.1,A=0.2Le=2Pr=0.71

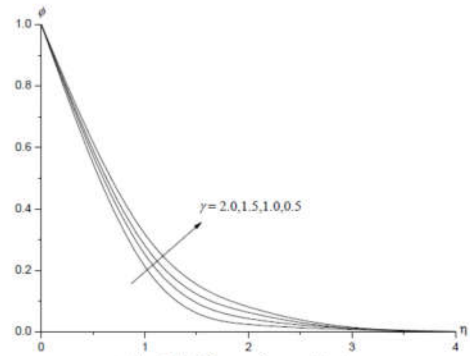

Fig.6d Effect of γ on ϕ(η)
G=2M=0.5,m=0.5,N=0.5,Nr=0.5,Nt=0.5,Nb=0.5,Q1=0.5, A1=0.1,B1=0.1,fw=0.2s=0.1,A=0.2Le=2Pr=0.71

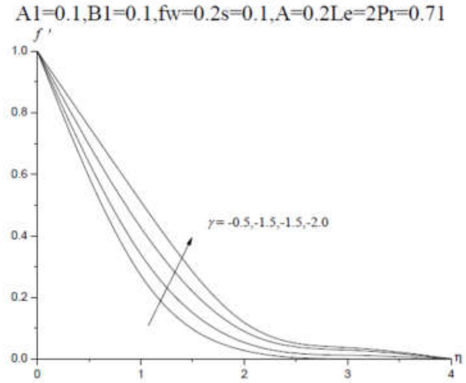

Fig.7a Effect of γ on $f'(\eta)$
G=2,M=0.5,m=0.5,N=0.5,Nr=0.5,Nt=0.5,Nb=0.5,Q1=0.5, A1=0.1,B1=0.1,fw=0.2,s=0.1,A=0.2,Le=2,Pr=0.71

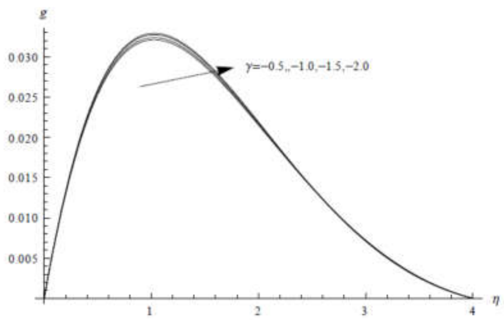

Fig.7b Effect of γ on g(η)
G=2M=0.5,m=0.5,N=0.5,Nr=0.5,Nt=0.5,Nb=0.5,Q1=0.5, A1=0.1,B1=0.1,fw=0.2s=0.1,A=0.2Le=2Pr=0.71

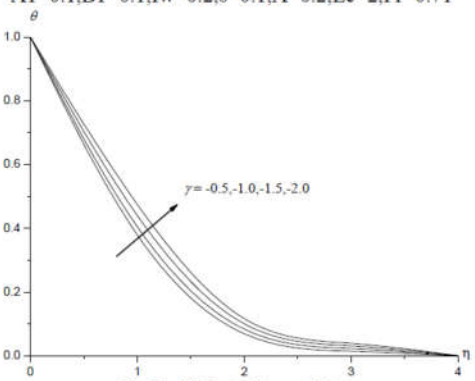

Fig.7c Effect of γ on θ(η)
G=2M=0.5,m=0.5,N=0.5,Nr=0.5,Nt=0.5,Nb=0.5,Q1=0.5, A1=0.1,B1=0.1,fw=0.2s=0.1,A=0.2Le=2Pr=0.71

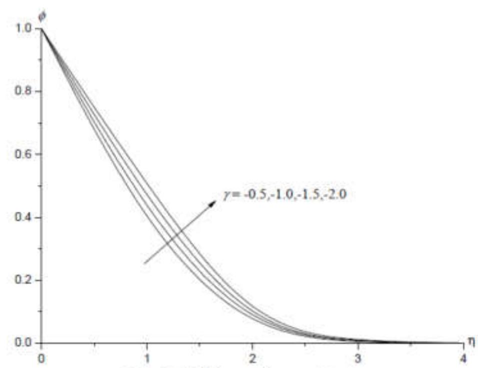

Fig.7d Effect of γ on ϕ(η)
G=2M=0.5,m=0.5,N=0.5,Nr=0.5,Nt=0.5,Nb=0.5,Q1=0.5, A1=0.1,B1=0.1,fw=0.2s=0.1,A=0.2Le=2Pr=0.71

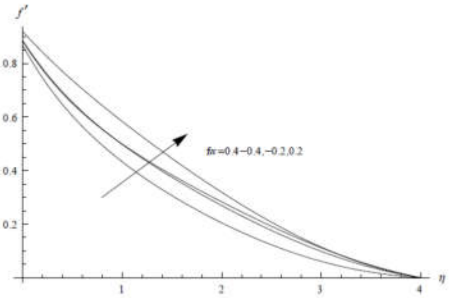

Fig.8a Effect of fw on $f'(\eta)$
G=2,M=0.5,m=0.5,N=0.5,γ=0.5,Nr=0.5,Nt=0.5,Nb=0.5,Q1=0.5, A1=0.1,B1=0.1,s=0.1,A=0.2,Le=2,Pr=0.71

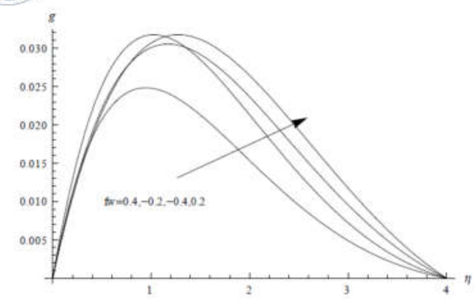

Fig.8b Effect of fw on g(η)
G=2M=0.5,m=0.5,N=0.5,γ=0.5,Nr=0.5,Nt=0.5,Nb=0.5,Q1=0.5, A1=0.1,B1=0.1,s=0.1,A=0.2Le=2Pr=0.71

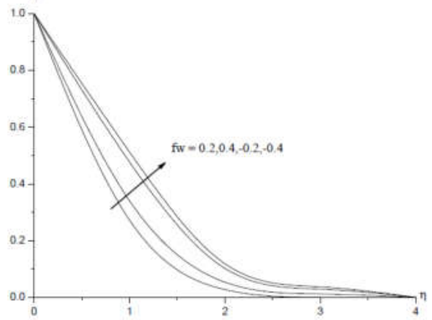

Fig.8c Effect of fw on θ(η)
G=2M=0.5,m=0.5,N=0.5,γ=0.5,Nr=0.5,Nt=0.5,Nb=0.5,Q1=0.5, A1=0.1,B1=0.1,s=0.1,A=0.2Le=2Pr=0.71

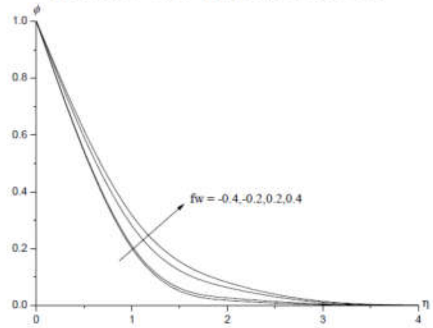

Fig.8d Effect of fw on ϕ(η)
G=2M=0.5,m=0.5,N=0.5,γ=0.5,Nr=0.5,Nt=0.5,Nb=0.5,Q1=0.5, A1=0.1,B1=0.1,s=0.1,A=0.2Le=2Pr=0.71

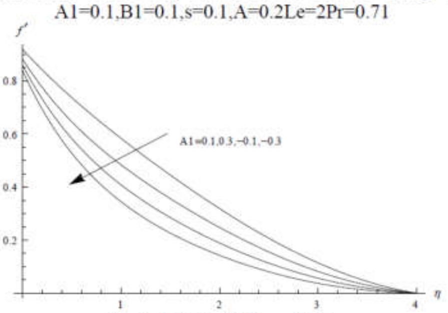

Fig.9a Effect of A1 on $f'(\eta)$
G=2,M=0.5,m=0.5,N=0.5,γ=0.5,Nr=0.5,Nt=0.5,Nb=0.5,Q1=0.5, B1=0.1,fw=0.2,s=0.1,A=0.2Le=2,Pr=0.71

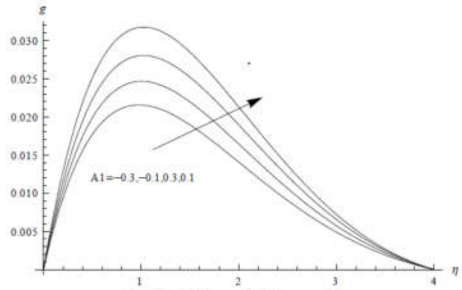

Fig.9b Effect of A1 on g(η)
G=2M=0.5,m=0.5,N=0.5,γ=0.5,Nr=0.5,Nt=0.5,Nb=0.5,Q1=0.5, B1=0.1,fw=0.2s=0.1,A=0.2Le=2Pr=0.71

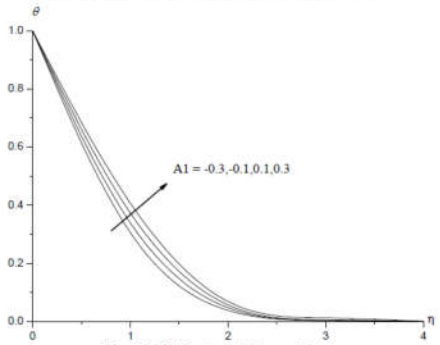

Fig.9c Effect of A1 on θ(η)
G=2M=0.5,m=0.5,N=0.5,γ=0.5,Nr=0.5,Nt=0.5,Nb=0.5,Q1=0.5, B1=0.1,fw=0.2s=0.1,A=0.2Le=2Pr=0.71

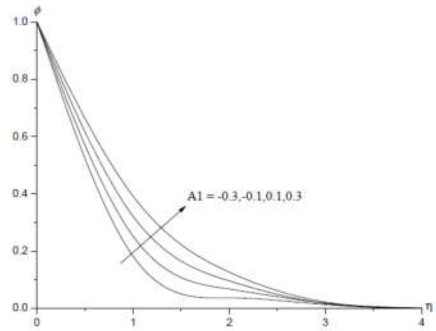

Fig.9d Effect of A1 on ϕ(η)
G=2M=0.5,m=0.5,N=0.5,γ=0.5,Nr=0.5,Nt=0.5,Nb=0.5,Q1=0.5, B1=0.1,fw=0.2s=0.1,A=0.2Le=2Pr=0.71

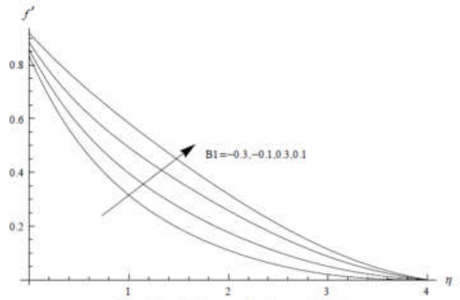

Fig.10a Effect of B1 on $f'(\eta)$
G=2,M=0.5,m=0.5,N=0.5,γ=0.5,Nr=0.5,Nt=0.5,Nb=0.5,Q1=0.5, A1=0.1,fw=0.2,s=0.1,A=0.2,Le=2,Pr=0.71

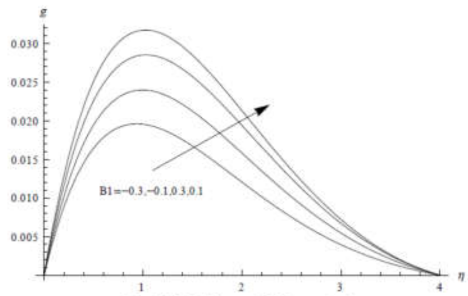

Fig.10b Effect of B1 on g(η)
G=2M=0.5,m=0.5,N=0.5,γ=0.5,Nr=0.5,Nt=0.5,Nb=0.5,Q1=0.5, A1=0.1,fw=0.2s=0.1,A=0.2Le=2Pr=0.71

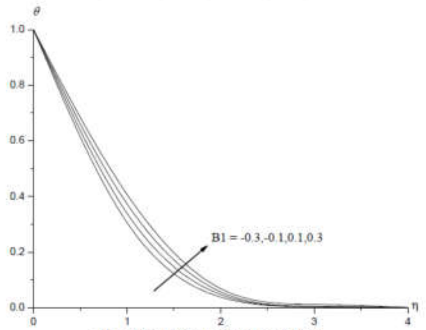

Fig.10c Effect of B1 on θ(η)
G=2M=0.5,m=0.5,N=0.5,γ=0.5,Nr=0.5,Nt=0.5,Nb=0.5,Q1=0.5, A1=0.1,fw=0.2s=0.1,A=0.2Le=2Pr=0.71

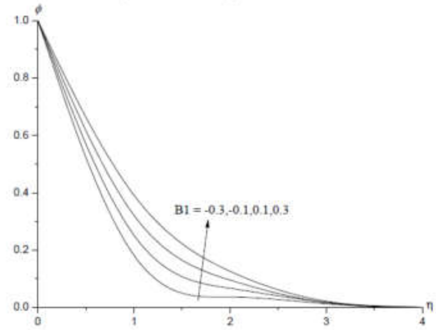

Fig.10d Effect of B1 on ϕ(η)
G=2M=0.5,m=0.5,N=0.5,γ=0.5,Nr=0.5,Nt=0.5,Nb=0.5,Q1=0.5, A1=0.1, fw=0.2s=0.1,A=0.2Le=2Pr=0.71

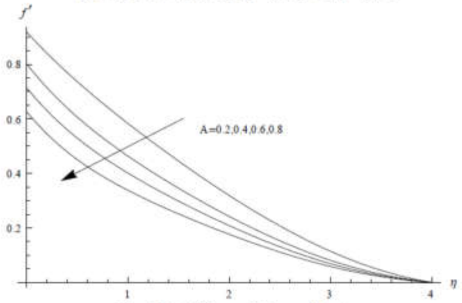

Fig.11a Effect of A on $f'(\eta)$
G=2,M=0.5,m=0.5,N=0.5,γ=0.5,Nr=0.5,Nt=0.5,Nb=0.5,Q1=0.5, A1=0.1,fw=0..2s=0.1,A=0.2,Le=2,Pr=0.71

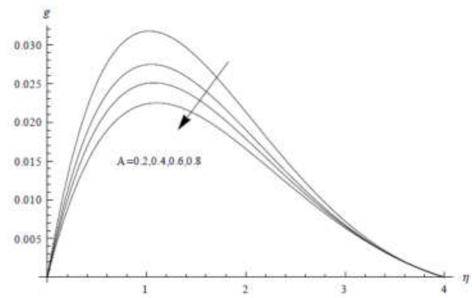

Fig.11b Effect of A on g(η)
G=2M=0.5,m=0.5,N=0.5,γ=0.5,Nr=0.5,Nt=0.5,Nb=0.5,Q1=0.5, A1=0.1,B1=0.1,fw=0.2s=0.1, Le=2Pr=0.71

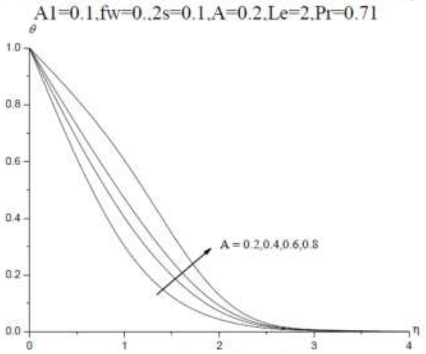

Fig.11c Effect of A on θ(η)
G=2M=0.5,m=0.5,N=0.5,γ=0.5,Nr=0.5,Nt=0.5,Nb=0.5,Q1=0.5, A1=0.1,B1=0.1,fw=0.2s=0.1, Le=2Pr=0.71

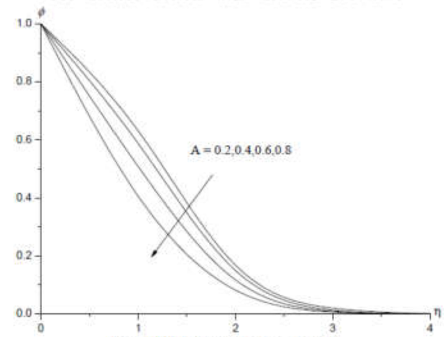

Fig.11d Effect of A on ϕ(η)
G=2M=0.5,m=0.5,N=0.5,γ=0.5,Nr=0.5,Nt=0.5,Nb=0.5,Q1=0.5, A1=0.1,B1=0.1,fw=0.2s=0.1, Le=2Pr=0.71

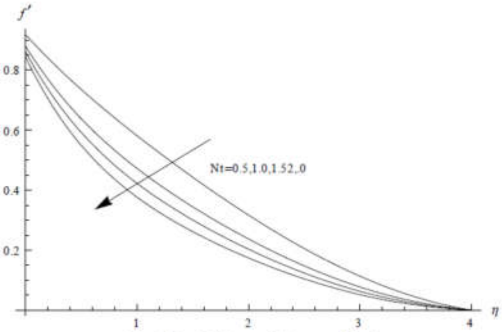

Fig.12a Effect of Nt on $f'(\eta)$
G=2,M=0.5,m=0.5,N=0.5,γ=0.5,Nr=0.5, Nb=0.5,Q1=0.5, A1=0.1,B1=0.1,fw=0.2,s=0.1,A=0.2,Le=2,Pr=0.71

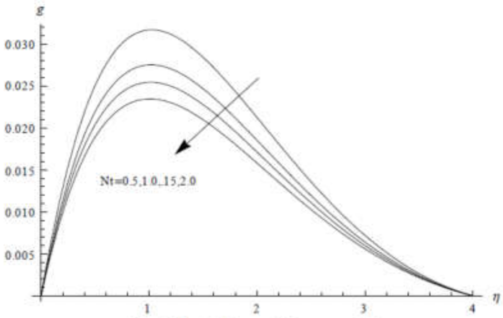

Fig.12b Effect of Nt on $g(\eta)$
G=2M=0.5,m=0.5,N=0.5,γ=0.5,Nr=0.5, Nb=0.5,Q1=0.5, A1=0.1,B1=0.1,fw=0.2s=0.1,A=0.2Le=2Pr=0.71

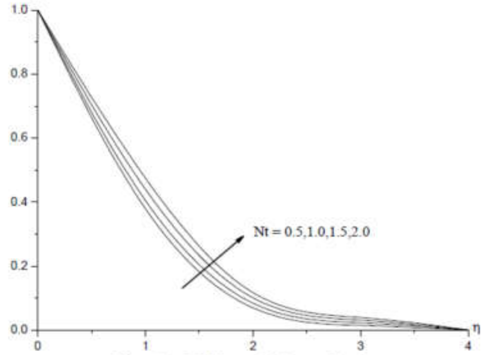

Fig.12c Effect of Nt on $\theta(\eta)$
G=2M=0.5,m=0.5,N=0.5,γ=0.5,Nr=0.5, Nb=0.5,Q1=0.5, A1=0.1,B1=0.1,fw=0.2s=0.1,A=0.2Le=2Pr=0.71

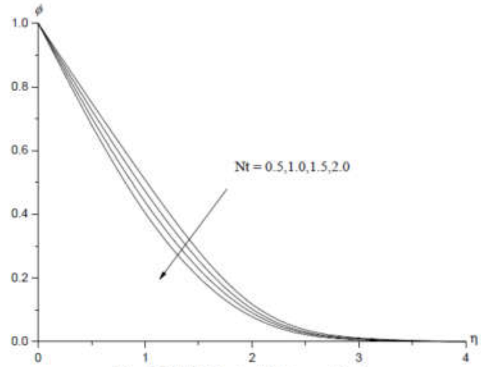

Fig.12d Effect of Nt on $\phi(\eta)$
G=2M=0.5,m=0.5,N=0.5,γ=0.5,Nr=0.5, Nb=0.5,Q1=0.5, A1=0.1,B1=0.1,fw=0.2s=0.1,A=0.2Le=2Pr=0.71

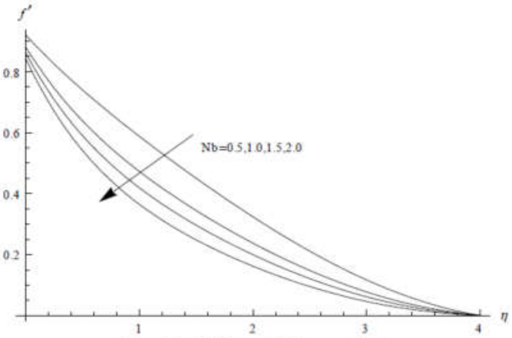

Fig.13a Effect of Nb on $f'(\eta)$
G=2,M=0.5,m=0.5,N=0.5,γ=0.5,Nr=0.5,Nt=0.5, Q1=0.5, A1=0.1,B1=0.1,fw=0.2,s=0.1,A=0.2Le=2,Pr=0.71

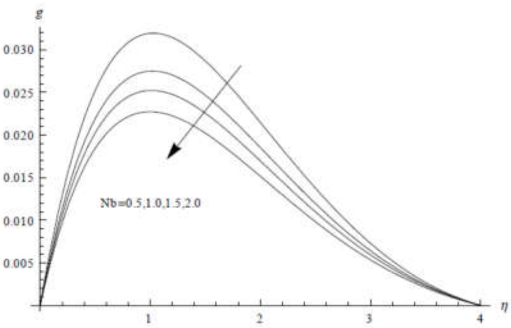

Fig.13b Effect of Nb on $g(\eta)$
G=2M=0.5,m=0.5,N=0.5,γ=0.5,Nr=0.5,Nt=0.5, Q1=0.5, A1=0.1,B1=0.1,fw=0.2s=0.1,A=0.2Le=2Pr=0.71

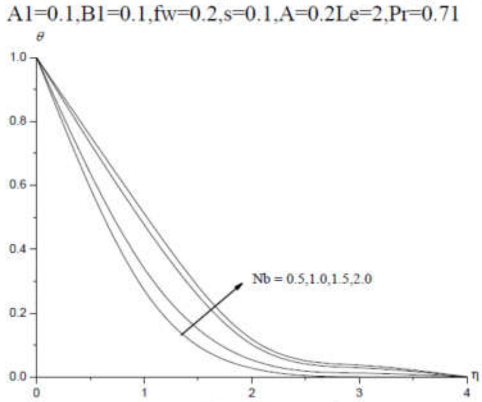

Fig.13c Effect of Nb on $\theta(\eta)$
G=2M=0.5,m=0.5,N=0.5,γ=0.5,Nr=0.5,Nt=0.5, Q1=0.5, A1=0.1,B1=0.1,fw=0.2s=0.1,A=0.2Le=2Pr=0.71

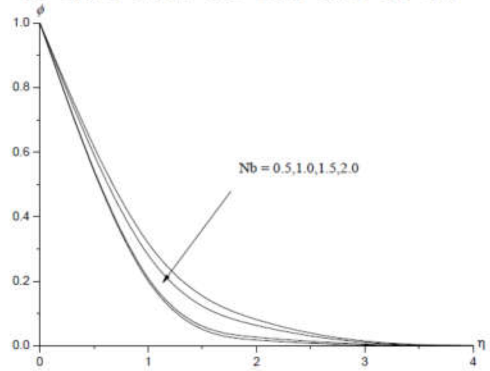

Fig.13d Effect of Nb on $\phi(\eta)$
G=2M=0.5,m=0.5,N=0.5,γ=0.5,Nr=0.5,Nt=0.5, Q1=0.5, A1=0.1,B1=0.1,fw=0.2s=0.1,A=0.2Le=2Pr=0.71

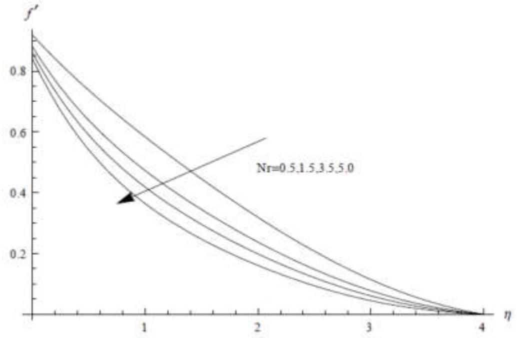

Fig.14a Effect of Nr on $f'(\eta)$
G=2M=0.5,m=0.5,N=0.5,γ=0.5, Nt=0.5,Nb=0.5,Q1=0.5, A1=0.1,B1=0.1,fw=0.2s=0.1,A=0.2Le=2Pr=0.71

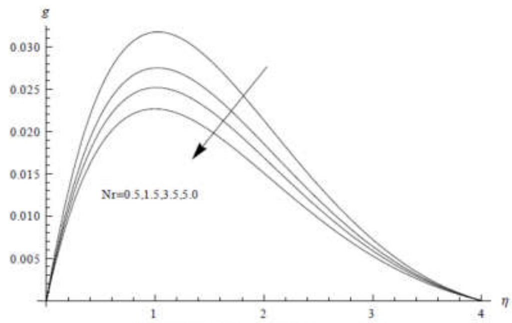

Fig.14b Effect of Nr on g(η)
G=2,M=0.5,m=0.5,N=0.5,γ=0.5, Nt=0.5,Nb=0.5,Q1=0.5, A1=0.1,B1=0.1,fw=0.2,s=0.1,A=0.2,Le=2,Pr=0.71

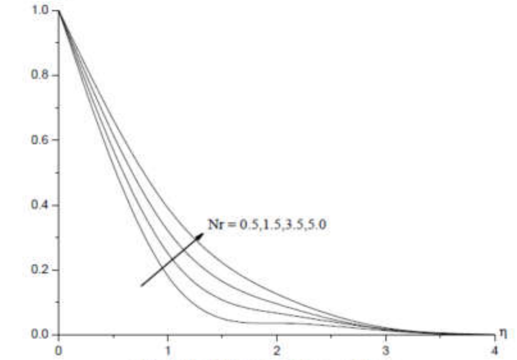

Fig.14c Effect of Nr on θ(η)
G=2M=0.5,m=0.5,N=0.5,γ=0.5, Nt=0.5,Nb=0.5,Q1=0.5, A1=0.1,B1=0.1,fw=0.2s=0.1,A=0.2Le=2Pr=0.71

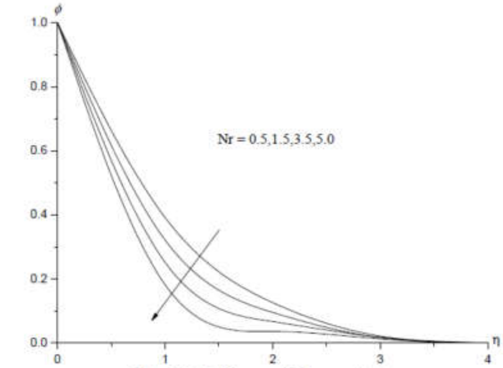

Fig.14d Effect of Nr on ϕ(η)
G=2M=0.5,m=0.5,N=0.5,γ=0.5, Nt=0.5,Nb=0.5,Q1=0.5, A1=0.1,B1=0.1,fw=0.2s=0.1,A=0.2Le=2Pr=0.71

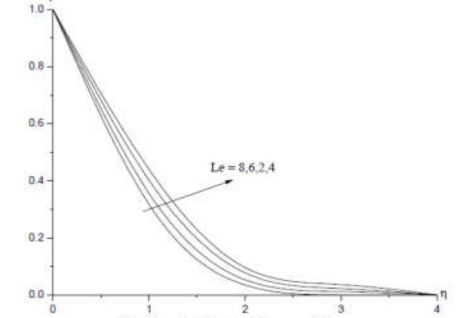

Fig.15a Effect of Le on $f'(\eta)$
G=2,M=0.5,m=0.5,N=0.5,γ=0.5,Nr=0.5,Nt=0.5,Nb=0.5,Q1=0.5, A1=0.1.B1=0.1.fw=0.2.s=0.1.A=0.2. Pr=0.71

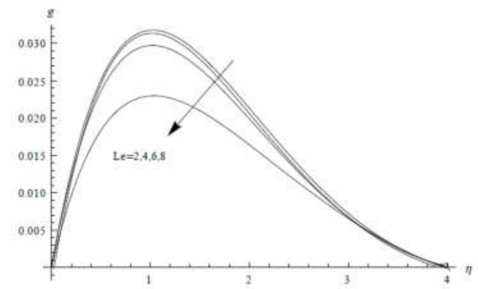

Fig.15b Effect of Le on g(η)
G=2M=0.5,m=0.5,N=0.5,γ=0.5,Nr=0.5,Nt=0.5,Nb=0.5,Q1=0.5, A1=0.1,B1=0.1,fw=0.2s=0.1,A=0.2 Pr=0.71

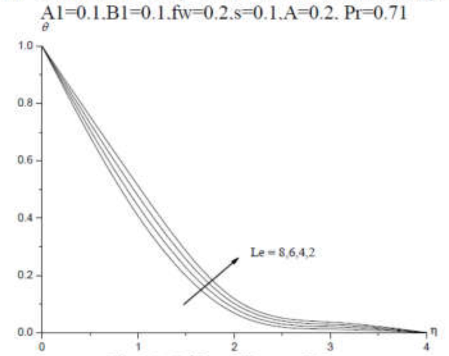

Fig.15c Effect of Le on θ(η)
G=2M=0.5,m=0.5,N=0.5,γ=0.5,Nr=0.5,Nt=0.5,Nb=0.5,Q1=0.5, A1=0.1,B1=0.1,fw=0.2s=0.1,A=0.2 Pr=0.71

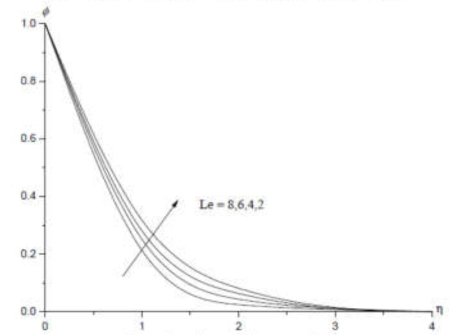

Fig.15d Effect of Le on ϕ(η)
G=2M=0.5,m=0.5,N=0.5,γ=0.5,Nr=0.5,Nt=0.5,Nb=0.5,Q1=0.5, A1=0.1,B1=0.1,fw=0.2s=0.1,A=0.2 Pr=0.71

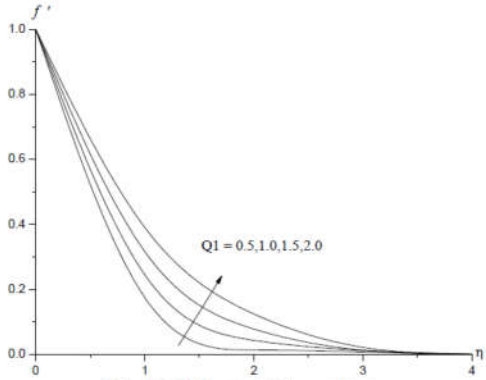

Fig.16a Effect of Q1 on $f'(\eta)$
G=2,M=0.5,m=0.5,N=0.5,γ=0.5,Nr=0.5,Nt=0.5,Nb=0.5,
A1=0.1,B1=0.1,fw=0.2,s=0.1,A=0.2,Le=2,Pr=0.71

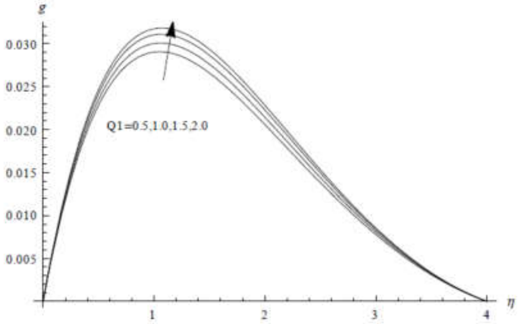

Fig.16b Effect of Q1 on g(η)
G=2M=0.5,m=0.5,N=0.5,γ=0.5,Nr=0.5,Nt=0.5,Nb=0.5,
A1=0.1,B1=0.1,fw=0.2s=0.1,A=0.2Le=2Pr=0.71

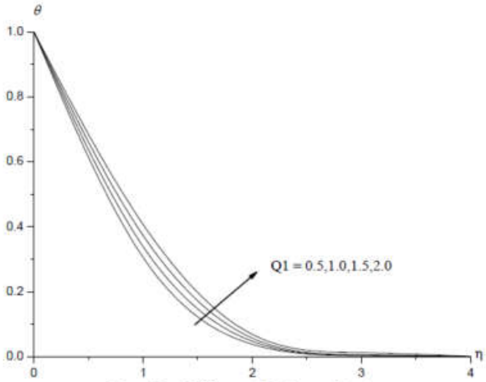

Fig.16c Effect of Q1 on θ(η)
G=2M=0.5,m=0.5,N=0.5,γ=0.5,Nr=0.5,Nt=0.5,Nb=0.5,
A1=0.1,B1=0.1,fw=0.2s=0.1,A=0.2Le=2Pr=0.71

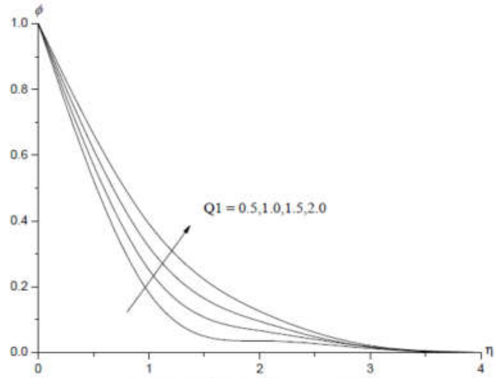

Fig.16d Effect of Q1 on ϕ(η)
G=2M=0.5,m=0.5,N=0.5,γ=0.5,Nr=0.5,Nt=0.5,Nb=0.5,
A1=0.1,B1=0.1,fw=0.2s=0.1,A=0.2Le=2Pr=0.71

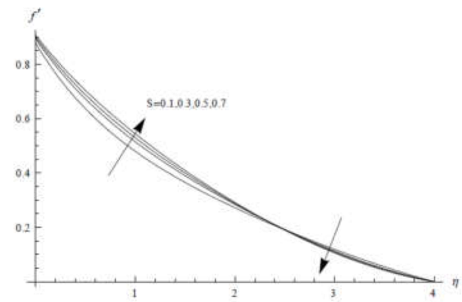

Fig.17a Effect of S on $f'(\eta)$
G=2,M=0.5,m=0.5,N=0.5,γ=0.5,Nr=0.5,Nt=0.5,Nb=0.5,Q1=0.5,
A1=0.1,B1=0.1,fw=0.2 ,A=0.2,Le=2,Pr=0.71

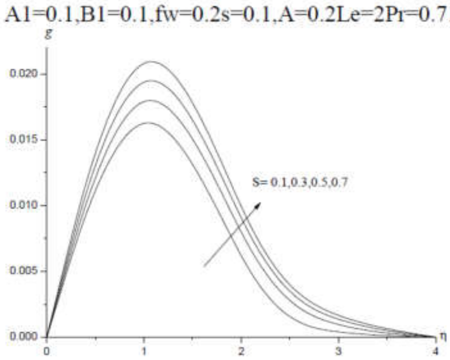

Fig.17b Effect of s on g(η)
G=2M=0.5,m=0.5,N=0.5,γ=0.5,Nr=0.5,Nt=0.5,Nb=0.5,Q1=0.5,
A1=0.1,B1=0.1,fw=0.2 A=0.2Le=2Pr=0.71

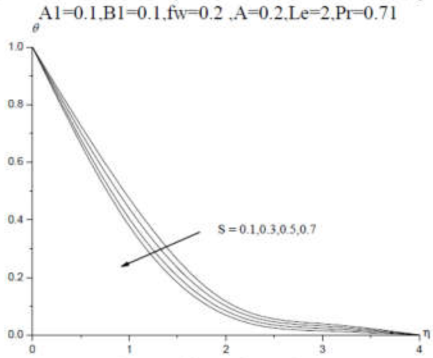

Fig.17c Effect of S on θ(η)
G=2M=0.5,m=0.5,N=0.5,γ=0.5,Nr=0.5,Nt=0.5,Nb=0.5,Q1=0.5,
A1=0.1,B1=0.1,fw=0.2 A=0.2Le=2Pr=0.71

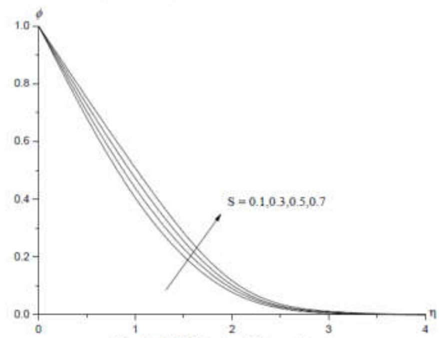

Fig.17d Effect of S on ϕ(η)
G=2M=0.5,m=0.5,N=0.5,γ=0.5,Nr=0.5,Nt=0.5,Nb=0.5,Q1=0.5,
A1=0.1,B1=0.1,fw=0.2 A=0.2Le=2Pr=0.71

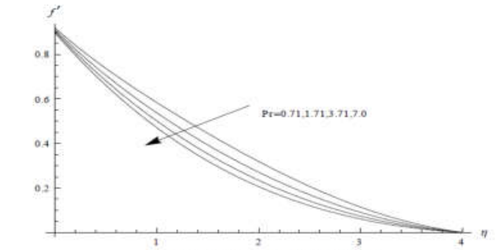

Fig.18a Effect of Pr on $f'(\eta)$
G=2,M=0.5,m=0.5,N=0.5,γ=0.5,Nr=0.5,Nt=0.5,Nb=0.5,Q1=0.5,
A1=0.1,B1=0.1,fw=0.2s=0.1,A=0.2Le=2

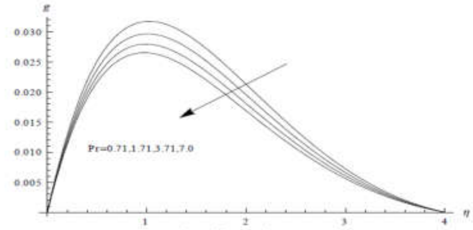

Fig.18b Effect of Pr on g(η)
G=2M=0.5,m=0.5,N=0.5,γ=0.5,Nr=0.5,Nt=0.5,Nb=0.5,Q1=0.5,
A1=0.1,B1=0.1,fw=0.2s=0.1,A=0.2Le=2

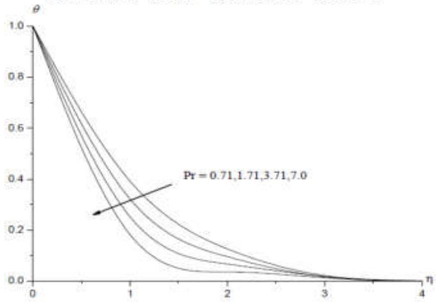

Fig.18c Effect of Pr on θ(η)
G=2M=0.5,m=0.5,N=0.5,γ=0.5,Nr=0.5,Nt=0.5,Nb=0.5,Q1=0.5,
A1=0.1,B1=0.1,fw=0.2s=0.1,A=0.2Le=2

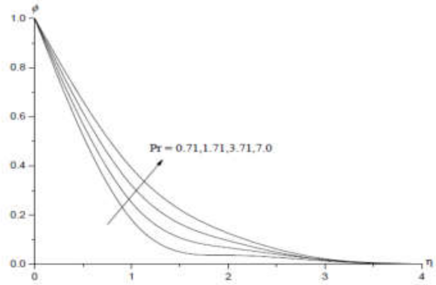

Fig.18d Effect of Pr on ϕ(η)
G=2M=0.5,m=0.5,N=0.5,γ=0.5,Nr=0.5,Nt=0.5,Nb=0.5,Q1=0.5,
A1=0.1,B1=0.1,fw=0.2s=0.1,A=0.2Le=2

Table 2. Skin friction ($\tau_{x,z}$), Nusselt number (Nu) and Sherwood number (Sh) at η=0.

Parameter		τx(0)	τz(0)	Nu(0)	Sh(0)	Parameter		τx(0)	τz(0)	Nu(0)	Sh(0)
G	2	-0.483977	0.0694066	0.349542	0.504789	Q1	0.5	-0.483977	0.0694066	0.349542	0.504912
	4	-0.100591	0.0820878	0.382073	0.467281		1.0	-0.463611	0.070822	0.278006	0.543933
	6	0.241407	0.0912561	0.407879	0.438571		1.5	-0.436322	0.0726269	0.177027	0.600699
	10	0.556184	0.0985752	0.42969	0.415021		2.0	-0.39782	0.0750093	0.0233935	0.690613
M	0.5	-0.483977	0.0694066	0.349542	0.504789	A1	0.1	-0.483977	0.0694066	0.349542	0.504789
	1.0	-0.572185	0.128783	0.341989	0.514017		0.3	-0.492179	0.0688587	0.381045	0.485993
	1.5	-0.97423	0.304521	0.309076	0.557059		-0.1	-0.475554	0.0699641	0.317287	0.523876
	2.0	-1.48659	0.433357	0.27618	0.60762		-0.3	-0.466466	0.0705597	0.282579	0.544242
m	0.5	-0.483977	0.0694066	0.349542	0.504789	B1	0.1	-0.483977	0.0694066	0.349542	0.504789
	1.0	-0.456488	0.0900069	0.351817	0.502012		0.3	-0.495325	0.0686233	0.390392	0.481641
	1.5	-0.433196	0.0858639	0.353794	0.499632		-0.1	-0.472371	0.0702566	0.308367	0.527602
	2.0	-0.414055	0.0658067	0.355451	0.49766		-0.3	-0.459239	0.0710876	0.262395	0.552459
N	0.5	-0.483977	0.0694066	0.349542	0.504789	fw	0.2	-0.483977	0.0694066	0.349542	0.504789
	1.0	-0.578884	0.0654463	0.340362	0.515319		0.4	-0.535555	0.0705495	0.354001	0.447598
	1.5	-0.669749	0.0614817	0.331536	0.525724		-0.2	-0.401463	0.0660397	0.342101	0.634743
	2.0	-0.852588	0.0529342	0.313698	0.547635		-0.4	-0.362187	0.0635857	0.338268	0.723401
γ	0.5	-0.483977	0.0694066	0.349542	0.504789	s	0.1	-0.449024	0.0723157	0.330509	0.450412
	1.0	-0.484566	0.0692611	0.376046	1.012272		0.3	-0.483977	0.0694066	0.349542	0.504789
	-0.5	-0.471093	0.0702458	0.228509	-0.585254		0.5	-0.517875	0.0665709	0.367613	0.555884
	-1.0	-0.526458	0.0686975	0.611238	0.89766		0.7	-0.598178	0.059879	0.40945	0.671983
Nr	0.5	-0.483977	0.0694066	0.349542	0.504789	A11	0.2	-0.483977	0.0694066	0.349542	0.504789
	1.5	-0.488572	0.0691024	0.366731	0.494791		0.4	-0.378122	0.0673927	0.345434	0.512674
	3.5	-0.492399	0.0688422	0.380565	0.486944		0.6	-0.315961	0.0661666	0.342946	0.517481
	5.0	-0.494079	0.0687261	0.386516	0.483619		0.8	-0.271602	0.0652699	0.341132	0.521001
Nt	0.5	-0.483977	0.0694066	0.349542	0.504789	Le	2	-0.483977	0.0694066	0.349542	0.504789
	1.0	-0.482676	0.0694939	0.345609	0.530214		4	-0.497987	0.0722976	0.3341524	0.623888
	1.5	-0.481507	0.0695743	0.341327	0.539335		6	-0.577943	0.0571841	0.2479852	0.858272
	2.0	-0.480329	0.0696559	0.336824	0.544577		8	-0.595975	0.0357662	0.1371801	0.933389
Nb	0.5	-0.483977	0.0694066	0.349542	0.504789	Pr	0.71	-0.483977	0.0694066	0.349542	0.504789
	1.0	-0.482335	0.0695337	0.341989	0.468686		1.71	-0.546223	0.0649748	0.582715	0.365458
	1.5	-0.480946	0.0696416	0.335917	0.441102		3.71	-0.59144	0.0617129	0.774534	0.237132
	2.0	-0.479586	0.0697473	0.330233	0.416704		7.00	-0.626671	0.0591773	0.942109	0.116486
Sr	0.5	-0.483977	0.0694066	0.349542	0.504789						
	0.75	-0.483987	0.0694077	0.349534	0.504789						
	1.0	-0.483999	0.069412	0.349529	0.504796						
	1.5	-0.484-22	0.0694211	0.349512	0.504819						

Conclusion

In this study a mathematical model for the unsteady MHD flow of a nanofluid generated by a stretching surface is analyzed. The effect of radioactive heat transfer and radiation absorption is also taken into account. Some of the salient features of this study are listed below.

- The effect of free convection parameter enhances the velocities while it decreases both temperature and concentration.
- Increasing values of buoyancy ratio decrease both velocities, temperature and increases concentration.
- Increasing values of magnetic parameter/porous parameter enhances temperature and reduces concentration while it decreases the velocities.
- The radiation parameter reduces velocities, concentration, enhances temperature.
- Velocities, concentration decrease and temperature increases with increasing values of Brownian motion and thermophoresis parameters.
- Increase in the Prandtl number decreases velocities and temperature while it increases the concentration.
- The heat source parameters (A1 and B1) decrease both velocities and enhance temperature and the nanofluid volume fraction.
- Increasing slip parameter (A) decreases velocities, nanofluid volume fraction, increases temperature.
- Velocities, temperature and nanofluid volume fraction increase with higher values of radiation Absorption.
- Temperature and concentration increase for increasing values of Lewis number while it increases velocities.
- Lesser the thermal diffusivity velocities, temperature, enhances nanofluid volume fraction. Our results are in excellent agreement with the previous published results in limiting cases.

References

1. Abd El-Aziz, M. 2009. Radiation effect on the flow and heat transfer over an unsteady stretching sheet. *Int. Commun. Heat Mass Transfer.* 36: 521-524.
2. Abd El-Aziz, M. 2010. Flow and heat transfer over an unsteady stretching surface with Hall Effect. *Meccanica*. 45: 97-109.
3. Abo-Eldahab, E.M. and Elbarbary, M.E. 2001. Hall current effect on magneto hydrodynamic free-convection flow past a semi-infinite vertical plate with masstransfer. *Int. J. Engg. Sci*. 39: 1641.
4. Abo-Eldahab, E.M. and Salem, A.M. 2004. Hall effects on MHD free convection flow of a non-Newtonian power-law fluid at a stretching surface. *Int. Commun. Heat Mass.* 31(3): 343-354.
5. Abo-Eldahab, E.M., Abd-El, Aziz, M. 2000. Hall and ion-slip effect on MHD free convective heat generating flow past a semi-infinite vertical flat plate. *Phs. Scripta*. 61: 344.
6. Ali, F.M., Nazar, R., Arifin, N.M. and Pop, I. 2011. Effect of Hall current on MHD mixed convection boundary layer flow over a stretched vertical flat plate. *Meccanica*. 46: 1103-1112.
7. Ali, M.E. 1994. Heat transfer characteristics of a continuous stretching surface. *Heat Mass Transfer.* 29: 227-234.
8. Bachok, N., Ishak, A. and Pop, I. 2010. Boundary layer flow of nanofluids over a moving surface in a flowing fluid. *Int. J. Thermal Sci.* 49: 1663-1668.
9. Bhattacharyya, K., Mukhopadhyay, S. and Layek, G.C. 2011. Slip effects on an unsteady boundary layer stagnation-point flow and heat transfer towards a stretching sheet. *Chinese Phys. Lett*. 28(9): 94702.
10. Buongiorno, J. 2006. Convective transport in nanofluids. *ASME J. Heat Transf*. 128: 240-250.
11. Chamkha, A.J., Aly, A.M. and Mansour, M.A. 2010. Similarity solution for unsteady heat and mass transfer from a stretching surface embedded in a porous medium with suction/injection and chemical reaction effects. *Chem. Eng. Commun.* 197: 846-858.
12. Choi, S.U.S. 1996. Enhancing thermal conductivity of fluids with nanoparticles, Developments and Applications of Non–Newtonian Flows. *FED*. 231(66): 99-105.
13. Dandapat, B.S., Santra, B. and Vajravelu, K. 2007. The effects of variable fluid properties and thermocapillarity on the flow of a thin film on an unsteady stretching sheet. *Int. J. Heat Mass Transf.* 50(5-6): 991-996.
14. Elbashbeshy, E.M.A. and Bazid, M.A.A. 2003. Heat transfer over an unsteady stretching surface with internal heat generation. *Appl. Math. Comp*. 138: 239-245.
15. Fang, T., Zhang, Z. and Yao, S. 2010. Slip magneto hydrodynamic viscous flow over a permeable shrinking sheet. *Chin. Phys. Lett*. 27(12): 124702.
16. Ganesan, P. and Palani, G. 2004. Finite difference analysis of unsteady natural convection MHD flow past an inclined plate with variable surface heat and mass flux. *Int. J. Heat Mass Transf.* 47 (19-20): 4449-4457.
17. Grubka, L.G. and Bobba, K.M. 1985. Heat transfer characteristics of a continuous stretching surface with variable temperature. J. *Heat Transf. Trans. ASME*. 107: 248-250.
18. Gupta, P.S. and Gupta, A.S. 1977. Heat and Mass Transfer on a stretching sheet with suction or blowing. *Can. J. Chem. J. Engg*. 55: 744-746.

19. Hamad, M.A.A. and Pop, I. 2011. Scaling transformations for boundary layer stagnation-point flow towards a heated permeable stretching sheet in a porous medium saturated with a nanofluid and heat absorption/generation effects. Transp. Porous Media. 87: 25-39.
20. Hayat, T., Saif, S. and Abbas, Z. 2008. The influence of heat transfer in an MHD second grade fluid film over an unsteady stretching sheet. *Phys. Lett. A*. 372: 5037- 5045.
21. Ishak, A. 2010. Unsteady MHD flow and heat transfer in over a stretching plate. *J. Appl. Sci*. 10(18): 2127-2130.
22. Jafar, K., Nazar, R., Ishak, A. and Pop, I. 2011. MHD Flow and Heat Transfer over stretching/shrinking sheets with external magnetic field, viscous dissipation and Joule effects. *Can. J. Chem. Eng.* 9999: 1-11.
23. Kakac, S. and Pramuanjaroenkij, A. 2009. Review of convective heat transfer enhancement with nanofluids. *Int. J. Heat Mass Transf.* 52: 3187-3196.
24. Khan, W. A. and Pop, I. 2010. Boundary layer flow of a nanofluid past a stretching sheet. *Int. J. Heat Mass Transf.* 53: 2477-2483.
25. Kuznestov, A.V. and Nield, D.A. 2009. Natural convective boundary– layer flow of a nanofluid past a vertical plate. *Int. J. Thermal Sci*. 20: 7-15.
26. Makinde, O.D. 2012. Entropy analysis for MHD boundary layer flow and heat transfer over a flat plate with a convective surface boundary condition. *Int. J. Energy.* 10(2): 142-154.
27. Mukhopadhyay, S. 2011. Heat transfer analysis of unsteady flow over a porous stretching surface embedded in a porous medium in presence of thermal radiation, *Acta Tech*. 56: 115-124.
28. Sakiadis, B.C. 1961. Boundary layer behaviour on a continuous solid surface. *AICHE J*. 7: 26-28.
29. Vajravelu, K. 1994. Flow and heat transfer in a saturated porous medium over a stretching surface. *Z. Agnew. Math. Mech*. 74: 605-614.